Estimation of Stratospheric Age Spectrum from Chemical Tracers

Mark R. Schoeberl, Anne R. Douglass
NASA Goddard Space Flight Center, Greenbelt, MD

Brian Polansky
Science Systems Applications Inc.
Greenbelt, Md.

Chris Boone, Kaley A. Walker, and Peter Bernath
Department of Chemistry
University of Waterloo
Waterloo, Ontario, Canada N2L 3G1

Abstract

We have developed a technique to diagnose the stratospheric age spectrum and estimate the mean age of air using the distributions of at least four constituents with different photochemical lifetimes. We demonstrate that the technique using a 3D CTM and then apply the technique to OMS tropical balloon observations, UARS CLAES January 1993 and ACE February-March, 2005 observations of CFC11, CFC12, CH_4 and N_2O. Our results using the ACE and OMS data are generally in agreement with mean age of air estimates from the chemical model and from observations of SF_6 and CO_2; however, the UARS derived mean age estimates show an intrusion of very young tropical air into the mid-latitude stratosphere. The UARS CLAES values of F11 and F12 appear to be significantly higher than ACE and model values and bias our lower stratospheric estimates of the age derived from UARS data toward younger values.

1. Introduction

The concept of the age-spectrum for trace gas transport [Kida, 1983; Hall and Plumb, 1994] has improved interpretation of the processes that lead to the observed distribution of stratospheric and oceanic minor constituents. The age-spectrum (sometimes called the boundary Green's function in oceanography) is the probability distribution of transit times for irreducible parcels between the source and the sample point within the interior of the domain. The age-spectrum thus links the boundary sources of constituents with the distribution within the interior.

The utility of the age-spectrum has been demonstrated for both the stratosphere [Waugh and Hall, 2002] and the ocean [Wunsch, 2002, Haine and Hall, 2002]. The application of this concept to the ocean and the stratosphere results from the fact that the boundary source region can be easily localized. For the stratosphere the boundary source region is the tropical tropopause. For the ocean, the boundary source region is the bottom water formation region in the North Atlantic.

The age-spectrum, although easily computed using a numerical model, cannot be directly observed. Nonetheless, the age-spectrum leaves its imprint on the observed tracer distribution. For example, the measurement of a tracer whose concentration at the boundary increases linearly with time automatically provides the first moment of the age-spectrum – the mean age. In the stratosphere, both CO_2 and SF_6 observations have been used to estimate the mean age [Waugh and Hall, 2002], and because of this property, tracers with a linearly increasing source are sometimes called clock tracers. Long records of nearly-inert tracers can also be used to estimate the age-spectrum [Johnson et al. 1999] but we do not have long reliable records of most observed tracers.

Additional information on the age-spectrum can be obtained from non-clock tracers. Schoeberl et al. [2000] noted this possibility for stratospheric constituents, and Hall et al. [2002] have estimated the oceanic age-spectrum using pairs of tracers with different source histories. In this paper, we further develop a technique to estimate the stratospheric age-spectrum from chemically active tracers. The idea is simple. Tracers with different lifetimes provide information about a different part of the distribution of transit times. Short-lived tracers are sensitive only to the rapid transit times since they are depleted after spending a short time in the stratosphere while long-lived tracers are more sensitive to the longer transit times. Roughly speaking with N tracers of different lifetimes we can obtain N independent pieces of information about the age-spectrum.

Our approach for reconstructing the stratospheric age-spectrum is as follows. The age-spectrum is assumed to follow the analytic solution of Hall and Plumb [1994]. This assumption has been verified by numerical models [Waugh et al., 1997, Schoeberl et al., 2000, Waugh and Hall, 2002]. Haine and Hall [2002] also used this approach to estimate ocean age-spectrum using observed tracers. However, we have modified the analytic age-spectrum by adding a tracer time lag that is required in the less diffusive stratospheric circulation.

To test our methodology, we use a stratospheric chemical transport model (CTM) to calculate the age-spectrum. We also compute the distribution of artificial tracers with a path independent lifetime and the distribution of chemically active tracers. We then test the age-spectrum reconstruction method by reproducing the age-spectrum using the model tracers. Next, we reconstruct the age-spectrum using the observed tracers from the Observations of the Middle Stratosphere (OMS) tropical balloon flights [Andrews et al. 2001], the Cryogenic Limb Array Etalon Spectrometer (CLAES) [Roche et al. 1993] flown aboard the Upper Atmosphere Research Satellite (UARS) and the Atmospheric Chemistry Experiment (ACE) observations [Bernath et al. 2005]. In the next section we briefly describe the methodology. Our results are described in the subsequent sections.

2.0 Computing the Mean Age and the Age-spectrum

The simplest method to compute the age-spectrum is to release a pulse (a delta function) of stratospherically inert tracer at the tropopause and allow it to disperse throughout the interior domain. Tracer loss only occurs in the troposphere. At a given point within the model domain, the graph of the concentration versus time is equivalent to the probability distribution function (PDF) of transit times for a stationary circulation. Hall and Waugh [1997] report the age-spectrum and mean age distributions for two general circulation models using this method.

It is important to recognize that for non-stationary flows the pulse-method of computing the age-spectrum cannot generate the instantaneous spectrum. For example, the pulse will travel through the tropical lower stratosphere first before propagating to the mid-latitude and polar stratospheres. Thus for non-stationary flows the resultant age-spectrum in the tropics will characterize flow conditions at the beginning of the integration period. Likewise the spectrum of the extra-tropics will be characterized by flow conditions over most of the integration period. As a result, calculations of the mean-age using the results from a pulse will not be exactly equivalent to the mean age using a clock tracer.

The chemical transport model (CTM) used in this study has been described by Douglass et al. [2003] and Schoeberl et al. [2003]. The model resolution is 2^{o} latitude by 2.5^{o} longitude with 28 pressure levels extending to 0.65 hPa. Here the CTM is driven by the GEOS-4 general circulation model (GCM) winds, not the data assimilation system winds discussed in Douglass et al., [2003]. The GCM driven CTM shows good tropical isolation of the lower stratosphere [Schoeberl et al., 2003] and compares well with observed tracer fields [Douglass et al., 2003]. To get the age-spectrum numerically, we integrate this model forward for 20 years after initiating a one-day square wave pulse at the tropical tropopause. The spectrum results from sampling the model every 30 days from the beginning of the integration. We also integrate a clock tracer (a linearly increasing surface source) and a series of seven radioactive tracers with lifetimes of 0.1, 0.3, 0.5, 1.0, 3.0, 5.0, and 7.0 years. The radioactive tracers have path independent loss rates thus their concentration is only a function of the transit time from the tropical tropopause. All of the chemical and radioactive tracer experiments were run for 20 years.

2.1 The Mean Age

The mean age, Γ, is defined as

$$\Gamma = \int_0^\infty tG(\bar{x}_0, \bar{x}, t)dt \qquad (1)$$

where $G(\bar{x}_0, \bar{x}, t)$ is the Green's function or the age-spectrum.While the concept is clear, various computations of the mean age can show subtle yet important differences. Fig. 1 shows the January mean age generated using the pulse and two clock-tracers. The Clock A tracer value is incremented at the surface (except at the start where clock is set to the same value everywhere) with no chemical loss at the domain interior. The Clock B tracer value is reset to the current date within the troposphere at each time step, this is equivalent to having a fast chemical loss in the troposphere.

While the mean ages for the three experiments are similar in basic structure, there are some differences. The differences appear to result from the differences in forcing and the chemical loss. In the pulse experiment, the pulse originates at the tropopause. Chemical loss occurs below the tropopause so that air re-circulating back through the tropopause has no tracer concentration. Thus, the pulse cannot return to the stratosphere to influence the age. This experiment is closer to Clock B and the mean ages are closer as well.

For the Clock A tracer, it would seem possible that air could re-circulate through the tropopause back into the stratosphere and bias the oldest air to be even older. Consistent with this argument, the Clock A ages are older than Clock B and the pulse mean ages

Returning to Figure 1 it is evident that for younger air, there is an additional bias between the pulse and clock experiments associated with air penetrating into the troposphere in the extra-tropics. For the pulse experiment, the pulse decays as it propagates into the troposphere due to the chemical loss localized in that region. For the Clock A and B experiments the continued forcing of the clock tracer tends to reset the tropospheric tracer values toward young air. As air is mixed into the lowermost extra-tropical stratosphere the clock values are biased toward young air.

2.2 The age spectrum from radioactive tracers

To test the machinery of estimating the age-spectrum using tracers we begin with tracers whose decay rate is a function only of age. We call these "radioactive' tracers. Using the CTM we have run radioactive tracers with lifetimes (not half–lives) of 0.1, 0.3, 0.5,1.0, 3.0, 5.0 and 7.0 years. This spread was chosen to cover the mean ages shown in Figure 1. Using these tracers we assume that the age-spectrum, *G*, has the functional form

$$G = \frac{z}{2\sqrt{\pi K(t - t_{off})^3}} \exp\left(\frac{z}{2H} - \frac{K(t - t_{off})}{4H^2} - \frac{z^2}{4K(t - t_{off})}\right) \qquad (2)$$

where z is the height (x in Eq. 1, x_0 is zero, and t is t-t_{off}) of the sample point, H is the atmospheric scale height (7 km), K is the diffusion coefficient, t is the age and t_{off} is the age offset. This form is equivalent to the analytic expression derived by Hall and Plumb [1994] with the addition of the age offset. In the original 1D Hall and Plumb model, G has a value everywhere for $t > 0$. In model calculations, the age-spectrum is usually offset by some small age value because it takes a while for the pulse to arrive advectively, and the diffusion of the material ahead of the pulse is not fast enough to produce an instantaneous response. Figure 2 illustrates this point, showing the pulse-generated age-spectrum at a variety of latitudes at 30 km. Note the age-spectrum offset at 30 km in the polar latitudes. We also note from Figure 2 that the age-spectrum generated by the model is quite similar to the analytic form.

To estimate the spectrum using tracers we use a multi-parameter least squares fit varying K, z, and t_{off} to generate test values of G. We then search for the minimum of the function F where

$$F = \sum (\mu_i - \mu^*_i)^2 \tag{3a}$$

$$\mu_i^* = \int e^{-\lambda t} G(t, x, x_o) dt \tag{3b}$$

where λ is the radioactive decay rate (1/lifetime) and μ is the volume mixing ratio. F can be thought of as a score for the best overall fit to the data, but the simple least squares difference is not the only way to score the fit. For example, F could be based upon percentage differences from the analytic form. That type of score would give more weight to fitting the tail of the age-spectrum distribution. Tests using both types of scores show that the form given by (3a) usually gives the best overall mean ages when compared to observations (discussed below with Figure 9).

Fig. 2 shows the spectrum fit generated using the radioactive tracers compared to the pulse generated spectrum at a series of latitudes at the altitude shown. The mean ages are also shown. Overall the procedure and the analytic form capture the major structural features of the age-spectrum. Figure 3 shows a comparison of the mean age estimated from the radioactive tracers compared to the mean age computed from the pulse experiment. We note that the radioactive tracer fit produces a slight bias, tending to over estimate the age of the oldest air, but otherwise the fit seems to produce reasonable results. The modal age (age of the maximum in the age spectrum) estimated from the radioactive tracers (not shown) also compares well with the pulse modal age.

2.3 The age spectrum from chemical tracers

For chemical constituents, the amount of photochemical loss depends on the accumulated exposure to photolyzing radiation or locally generated reactive compounds such as OH. For such "total exposure constituents" [McIntyre, 1992], the 1:1 relation between age and trace gas amount is blurred, and parcels with the same age may have different trace gas amounts, depending on the latitude and altitude range of their paths. The local loss of the

tracer by photolysis for species *i* can be written as $J_i = \int \sigma_i F d\upsilon$ where *F* is the local solar flux and σ_i is the molecular cross section. The integral takes place over all frequencies, ν. Because most long-lived tracers have cross sections with similar functional form, we can rewrite the expression above as $J_i = \beta_i \int \sigma F d\upsilon$. Now the photochemical exposure can be defined as $dn = (\int \sigma F d\nu) dt$ so that $d\mu = -\mu dn$ or in the case of OH loss $d\mu/dt = -k\mu[OH]$ where [OH] is the hydroxyl concentration and *k* is the reaction rate. If *F* were a constant, we would immediately recover the equivalent expression for the loss of a radioactive tracer. Schoeberl et al. [2000] showed that the average path approximation was valid for an ensemble of irreducible parcels with a given age. This approximation states that to first order we need consider only the average Lagrangian path of the irreducible fluid elements to the sample point, not the total spread of paths with same ages. Furthermore, because F increases so rapidly with height, we need only consider regions near the end of the path. Thus we can thus approximate $dn \approx \beta_i \overline{F}(y,z)\sigma dt$ where $\overline{F}$ is the average flux over the ensemble of average paths. Combining terms gives

$$\mu_i = \int e^{-\lambda_i(y,z)t} G(t,y,z,y_o,z_o) dt \qquad (4)$$

where $\lambda(y,z) = \beta_i \overline{F}(y,z)\sigma$. Thus the amount of the tracer is a function of the transit time with the loss coefficient a function of the final location. This result is consistent with Hall [2000] using the "leaky pipe" model of Neu and Plumb [1999]. Hall [2000] showed that the concentration of chemically active tracers was primarily a function of transit time because the longer transit times simply resulted in higher path altitudes and thus more rapid photochemical loss.

2.3.1 Model chemical tracers

Since we know μ_ι from the photochemical model and *G* from the pulse experiment, we can solve for the value of the path integrated photochemical loss frequency, λ in (4). This solution is obtained numerically at each point varying λ until the mixing ratio matches the model. Note that the path integrated photochemical loss frequency is not the same as the local photochemical loss frequency although they may be close to each other in the tropics. We compute the path integrated photochemical loss frequency for four source gases, the CFC's F11 (CCl_3F) and F12 (CCl_2F_2), N_2O and CH_4. Using (3a and 3b) we can compute the age-spectrum. Figures 4ad show the model values of the four trace gases and a computation of the same gases using (4). Values of λ^{-1} (roughly the decay time) are also shown in the figures. Note that λ^{-1} decreases rapidly with height in the tropics as expected from our approximations. λ^{-1} also decreases with latitude because the ensemble average path rises in the tropics and then falls at higher latitudes leaving the signature of the highest altitude (highest *F* value) on the value of λ. As expected λ^{-1} values are smaller (decay times are faster) for the shorter-lived tracers.

The mean age computed from the chemical tracer is shown in Figure 3. Our method produces a mean age that is quite comparable to the pulse and radioactive tracer mean age – although there is slightly more variability. Recall that with the radioactive tracer experiment we have seven tracers to constrain the three variables needed to estimate the

age spectra. With the chemically active tracers, we only have four so it is not surprising that the fits are less tightly constrained. The sample age spectra generated using (3a) are shown in Figure 2. The agreement with both the pulse age spectra and the radioactive trace gas spectra is good.

2.4 Observations

2.4.1 OMS

OMS balloon flights [Andrews et al., 2001b; Ray et al., 1999] in the tropics provide in situ measurements of methane and N_2O. In addition, measurements of CO_2 and SF_6 as well as F11 and F12 were made. The former can be used to estimate the mean age of air. Our analysis focuses on the tropical balloon flight that was made at 7° S on Feb. 14, 1997. N_2O and CH_4 were both measured by Alias and ARGUS diode laser spectrometers.

2.4.2 ACE-FTS

The ACE satellite carries a solar occultation Fourier Transform Spectrometer (FTS) providing global coverage over roughly a month of operations [Bernath et al., 2005]. ACE-FTS retrieval algorithms provide a large number of trace gases including N_2O, CH_4, F11 and F12. Here we use version 2.2 data. The ACE-FTS retrieval method is discussed by Boone et al. [2005], and validation is underway. Initial validation comparisons for version 1.0 have been completed [e.g., Walker et al. 2005; McHugh et al. 2005].

2.4.3 UARS

As mentioned above we use the observations of CH_4, F11, F12 and N_2O from UARS CLAES. The validation of CLAES observations is discussed in Roche et al. [1996] and Nightingale et al. [1996]. We focus on January 1993 averaged observations. January 1993 includes a yaw cycle and both hemispheres are observed for approximately the same number of days.

2.4.4 Comparison of Observations and the Chemical Model

Figure 5a-d compare the model, ACE and UARS data. Although these comparisons are for different years and slightly different seasonal time periods, there are significant differences between ACE and UARS that are likely a result of instrumental issues. First we note, that, in general, ACE is close to the model values for all four of the trace gases. Near the tropical tropopause, the archived CLAES data shows local minima and a comparatively low bias which is unrealistic compared to tropical balloon borne observations of N_2O, CH_4 and other trace gases [Elkins et al., 1996; Ray et al., 1999; Boering et al. 1996; Andrews et al., 2001] and Halogen Occultation Experiment (HALOE) [Russell et al., 1993] CH_4 observations [Park et al., 1996]. This anomaly is probably due to the interference of Pinatubo aerosol and tropical clouds in the CLAES retrieval algorithm. To be fair, the CLAES instrument was not designed to provide quality data at these higher pressure levels.

The CLAES F11 and F12 measurements also show biases. F11 and F12 both have a much higher concentration in the stratosphere than seen by ACE, and ACE is slightly high biased compared to the model. A possible explanation for the F11 and F12 differences could be the change in F11 and F12 over the last decade. Climate Monitoring and Diagnostics Laboratory (CMDL) provide on line updates of surface F11 and F12 concentrations. The data show that F11 concentrations peaked around 1994 and have declined about 8% to the present. F12 peaked around 2002 with a nearly negligible decline since. Thus the very high values of CLAES F11 and F12 compared to ACE cannot be explained by differences in measurement times.

The third possible explanation is that 1993 was a very anomalous year with strong tropical upwelling, and a circulation modulated by both the phase QBO and the Pinatubo aerosol. We discuss this hypothesis further below.

2.5 Age estimates from Observations

To estimate the age-spectrum from observations we must make the assumption that the λ values computed using the model are valid for the observed distributions as well. This assumption could be a small source of error. The error is small because the least squares fit to the multiple tracers tends to reduce errors associated with information from a single tracer. This is especially true in the lower stratosphere where all four tracers provide information on the age-spectrum. In order to estimate the age error as a function of the variations in the trace gases, we have performed numerical experiments perturbing the tracer field and computing the age. We find that the system response is nearly linear, in other words if the tracer fields are increased by 10%, the mean age is increased by 10%.

Another assumption we make is that the tropospheric source gas amounts are time independent. This is not strictly true, but the tropospheric source variations are small. Between the UARS and ACE measurement periods, N_2O surface concentration has increased about 5%, methane by 3%, F11 and F12 peaked and are decreasing slowly as described below. Prior to the 1993 CLAES measurements, both F11 and F12 were increasing strongly. This build up would bias the age estimates toward older ages because the approach in computing the age assumes a constant source. As a result a lower trace gas concentration would be ascribed to photochemistry (and a longer stratospheric residence time) not lower source values. This bias will be present mostly in the lower stratosphere where the concentrations of F11 and F12 are highest. Thus for age of air at two years, we expect that the growth of CFC's will bias the lower stratospheric CLAES age estimate by 10% high - roughly the growth in CFCs between 1991 and 1993.

In the calculations shown below, the trace gas fields are normalized by the tropospheric values measured by OMS Argus instrument.

Figure 6a shows the normalized trace gas fields fromthe OMS tropical data. The trace gas fields are normalized by the tropospheric values measured by OMS Argus instrument. As seen if Figure 5c there is a significant UARS F11 bias compared to the

other data sets. CLAES N_2O measurements also show significant bias especially below 24 km, both are lower than ACE and in situ data. ARGUS and Alias methane show some disagreement with each other above 20 km.

The age computations and the comparisons to estimated age from CO_2 and SF_6 are shown in Figure 6b. In general, the chemical age estimates using ACE and OMS data are in excellent agreement with CO_2 estimates. The SF_6 age is probably biased high compared to CO_2 age due to mesospheric loss of SF_6 as discussed by Waugh and Hall [2002]. The young age bias of the CLAES estimates can be attributed to high F11 concentrations.

Figure 7 shows the mean age computed from UARS CLAES and ACE data compared to the mean age computed from the same tracers using the model. The ACE data shows generally good agreement with the model in the lower stratosphere. However, above 30 km there is a detached region of young air in the southern hemisphere. This detached region is due to elevated values of methane compared to the model. In the Northern Hemisphere, very old are is present at high latitudes. This old air extends deep in to the lower stratosphere, as expected during winter. Also realistic is the break in this downward tongue of old air near 40 km as often occurs when the winter vortex begins to break up.

The mean age from UARS data shows several distinct features that contrast with the model. The most dramatic of these features the extension of very young air out of the tropical lower stratosphere into the Northern Hemisphere. The origin of this feature is clearly seen in the zonal mean CLAES trace gas measurements that show the extension northward out of the tropics (Fig. 5). O'Sullivan and Dunkerton [1997] also noted this feature in the CLAES N_2O. They attributed this northward extension to the additional tropical mid-latitude eddy interaction during the westerly phase of the quasi-biennial oscillation (QBO) in the lower stratosphere. The numerical model does not exhibit a QBO so variations in the isolation of the tropics with QBO phase are not produced in the model. The fact that this extension is so young is likely due to the high values of CLAES F11 and F12. The UARS values are between 20%-60% too high compared to ACE and OMS data, this would produce ages 20-60% too young. This extension of young air out of the tropics is probably real, but its age is underestimated by biases in the CLAES measurements.

Another distinct feature in the UARS age estimation is that it appears that young tropical air overlies older tropical air. This effect is the direct result of the reversed vertical gradient in tropical N_2O and F12 values occurring above the tropopause. Note that neither the model, OMS nor the ACE data show this feature so it is likely due to the CLAES retrievals which may have been contaminated by residual Pinatubo aerosol.

Fig. 8 compares the 20 km SF_6 and CO_2 derived mean ages composited by Waugh and Hall [2002] from a variety of data sources. The strong tropical isolation of young air is a common feature as evidenced by the strong age gradient with latitude. The model estimates of the mean age using the pulse, clock, radioactive and chemical tracers reasonably reproduce this feature although the middle latitude ages are all slightly

younger than the age estimated using CO_2. Age estimates using the ACE data also show reasonable agreement with the model. The age estimates using the CLAES data also show isolation of the tropics from the Southern Hemisphere, and the age in the Northern Hemisphere shows the intrusion of young air out of the tropics as discussed above and does not compare well with observations, ACE or the model.

Finally, Fig. 9 compares the 30 km age spectrum from the model using the four tracers (see Fig. 2) and the age spectrum diagnosed from the CLAES and ACE data. The structure of the ACE spectrum is quite similar to that calculated from model tracers with the exception that the spectrum is too narrow near the tropics. The CLAES spectrum is young biased at all latitudes compared to ACE and the model as also seen in Figs 7 and 8.

3.0 Summary and Discussion

A number of studies have sought to produce an estimate of the mean age of the stratosphere to diagnose the circulation and test models. However, the mean age is just the first moment of the age spectrum and for trace gases with finite chemical lifetime, the age spectrum itself is more useful. Depending on their lifetime, these chemically active gases may not be sensitive to the tail of the transit time distribution, which often strongly weights the mean age. Thus it would be useful to estimate the age spectrum from observed trace gases, and that is the goal of this study.

Using a multiple parameter least-squares fit we can estimate the age-spectrum from trace gas measurements. Hall et al. [2002] has used the same approach to estimate the age of deep ocean water from tracers. Our approach differs from Hall et al. [2002] in that we use a 3 parameter model of the spectrum and we use chemically active tracers rather than tracers with differing source histories. We first test the approach by generating an age-spectrum using a 3D GCM and then recovering the spectrum with tracers that have a path independent decay rate (radioactive tracers). Along the way we note that computations of the mean age, even using the same model, can be complicated by assumptions about tropospheric loss.

We test our age spectrum estimation method using chemically active tracers from the model. Because we do not have path information for the real atmosphere we assume that the chemical loss rate for the tracers is only a function of transit time. We argue that this approximation is reasonable since the photochemical loss increases with altitude so rapidly that longer transit times basically means that the irreducible parcels are reaching a higher altitude Hall [2000]. The parameterized chemical loss is computed from the model age-spectrum and trace gas concentration for CH_4, N_2O, F11 and F12.

We next extend our analysis to OMS in situ balloon observations, ACE satellite observations and UARS CLAES observation. The OMS data also provide estimates of mean age of air from CO_2 and SF_6. Our calculation of the mean age of air using the OMS tracers shows good agreement with the mean age estimated from CO_2. ACE tropical trace gas data also provide a good estimate of the mean age of air. CLAES data, on the other hand show significant biases between both ACE and OMS data. Broader

comparisons between ACE and CLAES data show CLAES F11 and F12 are biased too high while N_2O tropical concentrations are low. As a result of the F11 and F12 biases, our computed mean age using CLAES data is younger than suggested by the observations composited by Waugh and Hall [2002]. On the other hand, ACE data shows good agreement with CO_2 estimated ages in the lower stratosphere.

One interesting feature in the CLAES results is the apparent breakout of young air from the tropics into the lower stratosphere. While we think that our estimates of the age of this feature are too low, we note that O'Sullivan and Dunkerton [1997] discussed this unusual feature in the CLAES data as well and they attributed additional tropical-mid-latitude mixing associated with the westerly phase of the QBO. This result suggests that there may be important year-year age variation in the lower stratosphere.

Our approach requires three pieces of information to recover the age spectrum. At higher altitudes (above 30 km), it is clear that only observations of CH_4 and N_2O provide any information on the spectrum because F11 and F12 measurements are too noisy. Thus while mean age estimates appear to still be valid in this upper stratosphere, we note that the spectrum can become distorted. This problem can also occur at high winter latitudes where upper stratospheric are can descend into the lower stratosphere.

The approach we have developed here provides a quantitative method for simultaneous interpretation of many trace gas measurements. While the analytic form of the age-spectrum is somewhat simplified, trajectory and chemical transport model estimates of the age-spectrum [e.g. Schoeberl et al., 2002] show that the analytic form first suggested by Hall and Plumb [1994] with the addition of an offset captures most of the information.

Although we have used only four tracers, tests with the radioactive tracers suggest that more robust results would be obtained with additional tracers with different lifetimes including clock tracers. For example, the four tracers used here plus SF_6 and perhaps some even shorter-lived halocarbons would provide a useful basis set. These measurements could be obtained from ACE and Aura measurements of stratospheric composition.

Acknowledgements

This work was performed while the first author spent a few months visiting Oregon State University. He would like to thank the College of Oceanic and Atmospheric Sciences for their hospitality and the faculty for their interest. Darryn Waugh and two anonymous reviewers made very helpful comments on the manuscript, and Darryn provided us with the OMS data. Funding for ACE is provided by the Canadian Space Agency and the Natural Sciences and Engineering Research (NSERC) of Canada. Support at Waterloo was also provided by the NSERC-Bomem-CSA-MSC Industrial Research Chair in Fourier Transform Spectroscopy.

References

Andrews, A. E., et al., Mean ages of stratospheric air derived from in situ observations of CO_2, CH_4, and N_2O, J. Geophys. Res., 106, 32,295–32,314, 2001.

Bernath, P. F., et al., Atmospheric Chemistry Experiment (ACE) mission overview, Geophys. Res. Lett., 32, doi:10.1029/2005GL022386, 2005.

Boering, K. A., S. C. Wofsy, B. C. Daube, H. R. Schneider, M. Loewenstein and J. R. Podolske, Stratospheric transport rates and mean age distributions derived from observations of atmospheric CO_2 and N_2O, Science, 274, 1340-1343, 1996.

Boone, C. D., et al., Retrievals for the Atmospheric Chemistry Experiment Fourier Transform Spectrometer, Applied Optics, (in press) 2005.

Douglass, A. R., M. R. Schoeberl and R. B. Rood, Evaluation of transport in the lower tropical stratosphere in a global chemistry and transport model, J. Geophys. Res., 108, doi:101029/2002JD002696, 2003.

Elkins, J. W. et al., Airborne gas chromatograph for in situ measurements of long-lived species in the upper troposphere and lower stratosphere, Geophys. Res. Lett., 101, 16757-16770, 1996.

Hall, T. M., Path histories and timescales in stratospheric transport: Analysis of an idealized model, J. Geophys. Res., 105, 22,811–22,823, 2000.

Haine, T. W. N. and T. M. Hall, A generalized transport theory: Water-mass composition and age, J. Phys. Oceanogr., 32, 1932-1946, 2002.

Hall, T. M., and R. A. Plumb, Age as a diagnostic of stratospheric transport, J. Geophys. Res. 99, 1059-1070, 1994.

Hall, T. M., D. W. Waugh, K. A. Boering and R. A. Plumb, Evaluation of transport in the stratospheric models, J. Geophys. Res., 104, 18815-188839, 1999.

Hall, T. M., T. W. Haine, and D. W. Waugh, Inferring the concentration of anthropogenic carbon in the ocean from tracers, Global Biogeochem. Cycles, 16, doi:10.1029/2001GB001835, 2002.

Johnson D. G., et al., Stratospheric age spectra derived from observations of water vapor and methane, J. Geophys. Res., 104, 21,595–21,602, 1999.

Kida, H., General circulation of air parcels and transport characteristics derived from a hemispheric GCM, Part 2, Very long-term motions of air parcels in the troposphere and stratosphere, J. Meteorol. Soc. Jpn., 61, 510-522, 1983.

McHugh, M. et al., Comparison of atmospheric retrievals from ACE and HALOE, Geophys. Res Lett. 32, L15S10, doi:10.1029/2005GL022403, 2005.

McIntyre, M. E., Atmospheric Dynamics: Some fundamentals, with Observational Implications, in The Use of EOS for the Study of Atmospheric Physics, Proceedings of the International School of Physics, "Enrico Fermi" Course 115, G. Visconti and J. Gille, eds., North Holland, NY, 313-386, NATO Summer School, 1992.

Nightingale, R. W. et al., Global CF_2C1_2 measurements by UARS cryogenic limb array etalon spectrometer: Validation by correlative data and a model, J. Geophys. Res., 101, 9711-9736, 1996.

Neu, J. L., and R. A. Plumb, Age of air in “leaky pipe” model of stratospheric transport, J. Geophys. Res., 104, 19,243–19,255, 1999.

O’Sullivan, D and T. J. Dunkerton, Influence of the quasi-biennial oscillation on the global constituent distributions, J. Geophys. Res., 102, 21731-21743, 1997.

Park, J. H. et al. Validation of Halogen Occultation Experiment CH_4 measurements from the UARS, J. Geophys. Res., 101, 10,183-10,204, 1996.

Ray, E. A., et al., Transport into the Northern Hemisphere lowermost stratosphere revealed by in situ tracer measurements, J. Geophys. Res., 104, 26,565–26,580, 1999.

Roche, A. E, et al., Validation of CH_4 and N_2O measurements by the cryogenic limb array etalon spectrometer instrument on the upper atmosphere research satellite. J. Geophys. Res., 101, 9679-7710, 1996

Roche, A. E., et al., The cryogenic limb array etalon spectrometer (CLAES) on UARS: Experimental description and performance, J. Geophys. Res., 98, 10763-10776, 1993.

Russell, J. M. et al., The halogen occultation experiment, J. Geophys. Res., 98, 10777-10798, 1993.

Schoeberl, M. R., L. Sparling, A. Dessler, C. H. Jackman, and E. L. Fleming, A Lagrangian view of stratospheric trace gas distributions, J. Geophys. Res., 105, 1537–1552, 2000.

Schoeberl M. R., A. R. Douglass, Z. Zhu, and S. Pawson, A comparison of the lower stratospheric age spectra derived from a general circulation model and two data assimilation systems, J. Geophys. Res., 108, 4113, doi:10.1029/2002JD002652, 2003.

Walker, K.A., C.E. Randall, C.R. Trepte, C.D. Boone, and P.F. Bernath, Initial validation comparisons for the Atmospheric Chemistry Experiment (ACE-FTS), Geophys. Res. Lett. 32, L16S04, doi:10.1029/2005GL022388, 2005

Waugh, D.W., Hall, T.M., and T.W.N. Haine, Relationships among Tracer Ages, J. Geophys. Res., 108, 5, 10.1029/2002JC001325, 2003

Waugh, D. W. and T. M. Hall, Age of stratospheric air: Theory, observations and models, Revs. Of Geophys., 40, doi:10.1029/2000RG000101, 2002.

Waugh, D. W., et al., Three dimensional simulations of long lived tracers using winds from MACCM2, J. Geophys. Res., 102, 21493-21514, 1997.

Waugh, D.W., Vollmer M.K., Weiss, R.F., T.W.N. Haine and Hall, T.M., Transit time distributions in Lake Issyk-Kul, Geophys. Res. Lett., 29 (24), 10.1029/2002GL016201, 2002.

Wuench, C., Oceanic age and transient tracers: Analytical and numerical solutions, J. Geophys. Res., 107,10.1029/2001JC000797, 2002.

Figures

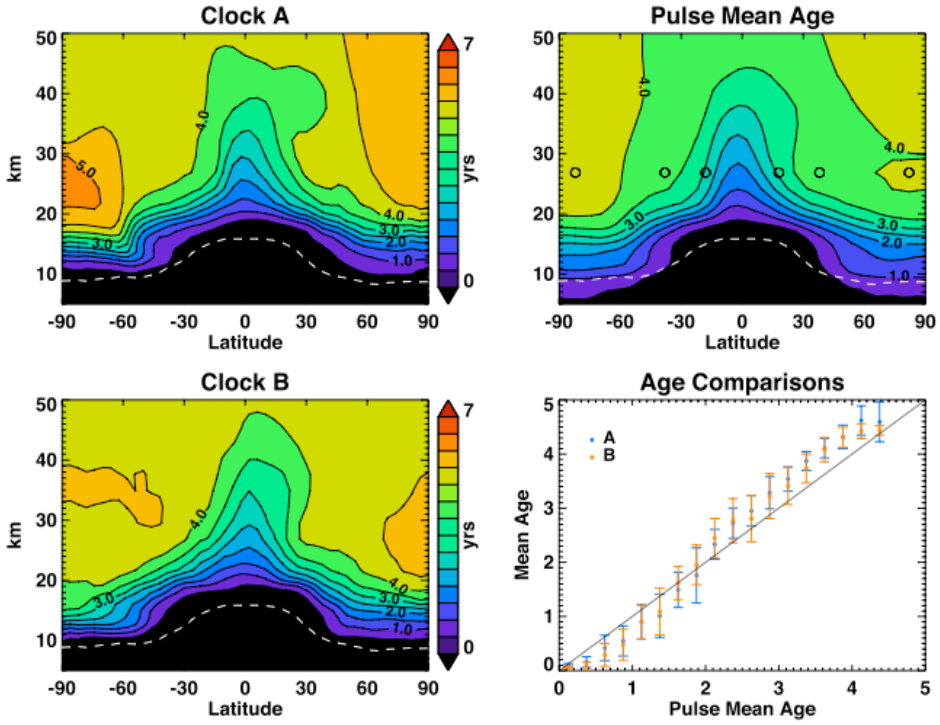

Figure 1. This figure shows the results of a January mean age calculation using two clock tracers (A and B) and the mean age computed from the pulse experiment. The two clock-tracer mean ages are plotted against the pulse experiment mean age at the lower right. Circles represent the mean value and the error bars indicate one standard deviation. See text for discussion. Small circles in the upper right figure show the location of the spectra shown in Figure 2.

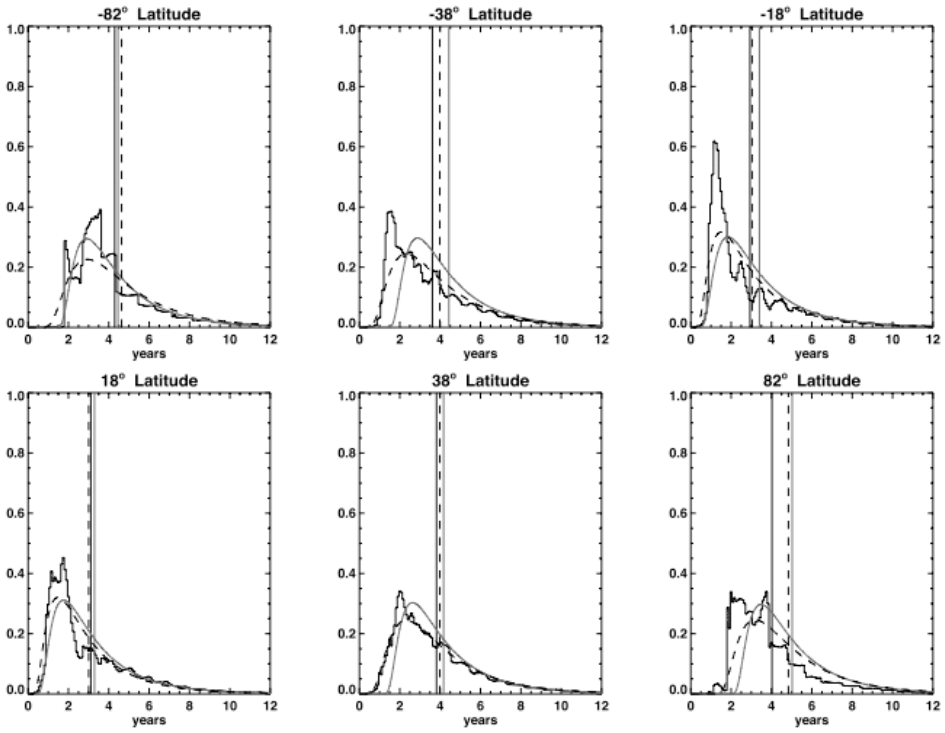

Figure 2. The age spectra computed from the model at 30 km and the latitude indicated in the graph title. Locations are shown in Figure 1. Solid lines show the model spectra. Gray (smooth) and dashed lines show the fit spectrum using the radioactive tracers and the four chemical constituents, respectively. Vertical lines show the mean ages.

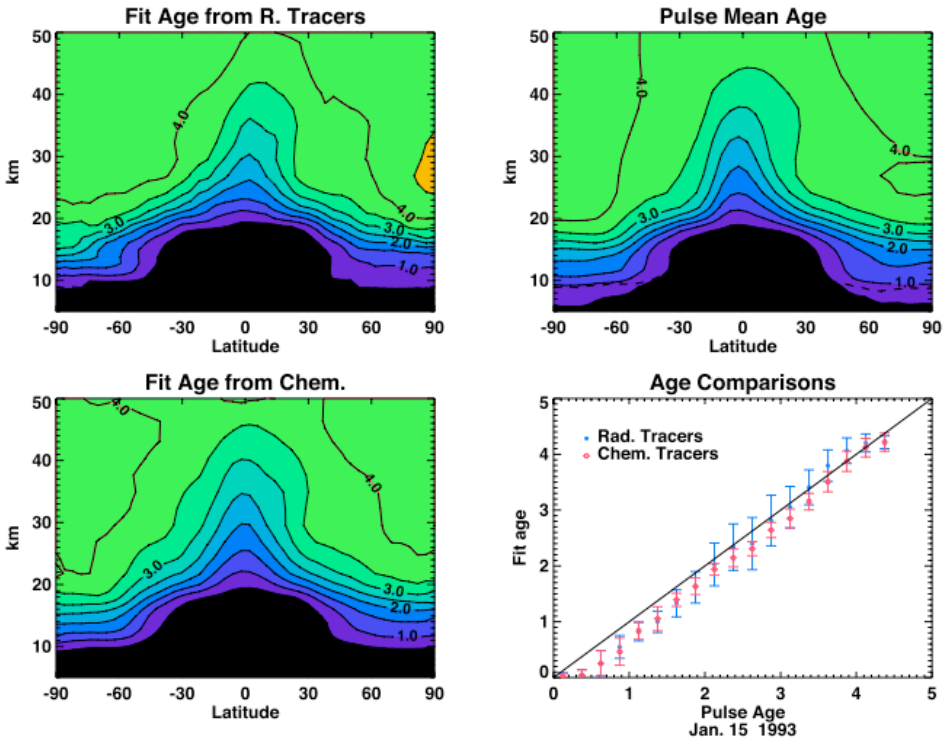

Figure 3. This figure shows the mean age from the pulse experiment compared to the mean ages estimated from the radioactive tracers and the chemical tracers. Also see Fig. 2.

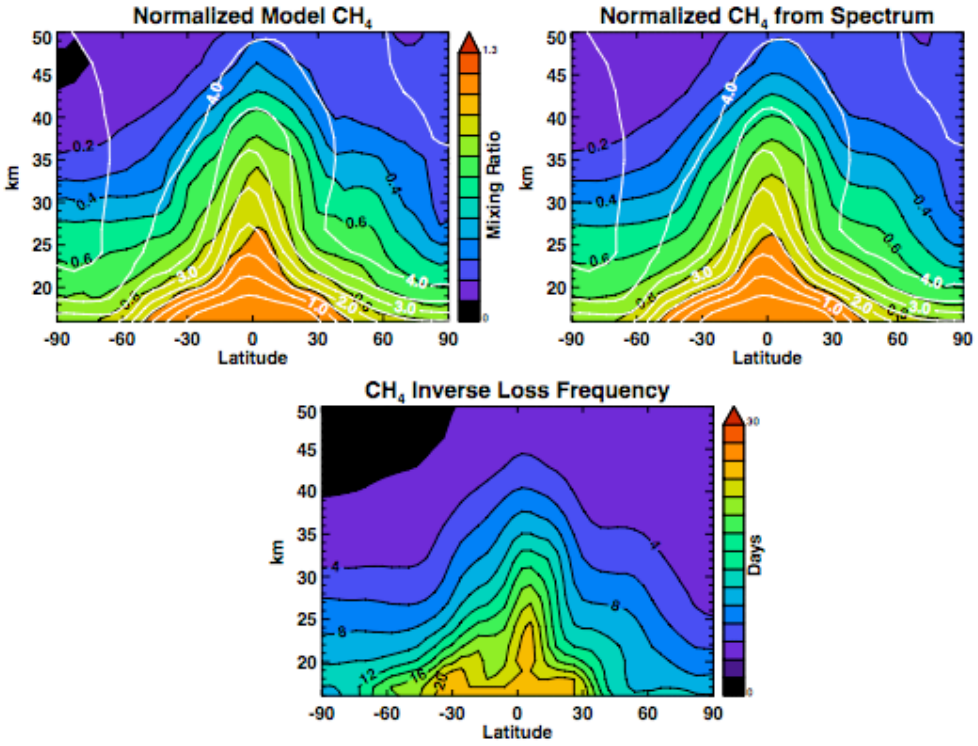

Figure 4a. The top left panel shows the normalized chemical model values for CH_4 averaged for January normalized to the peak value. The lower panel shows $\square^{1}$. The upper right panel shows the computed tracer amount using the age spectrum and the path integrated loss frequency, l. The mean age contours are shown over both upper figures in white.

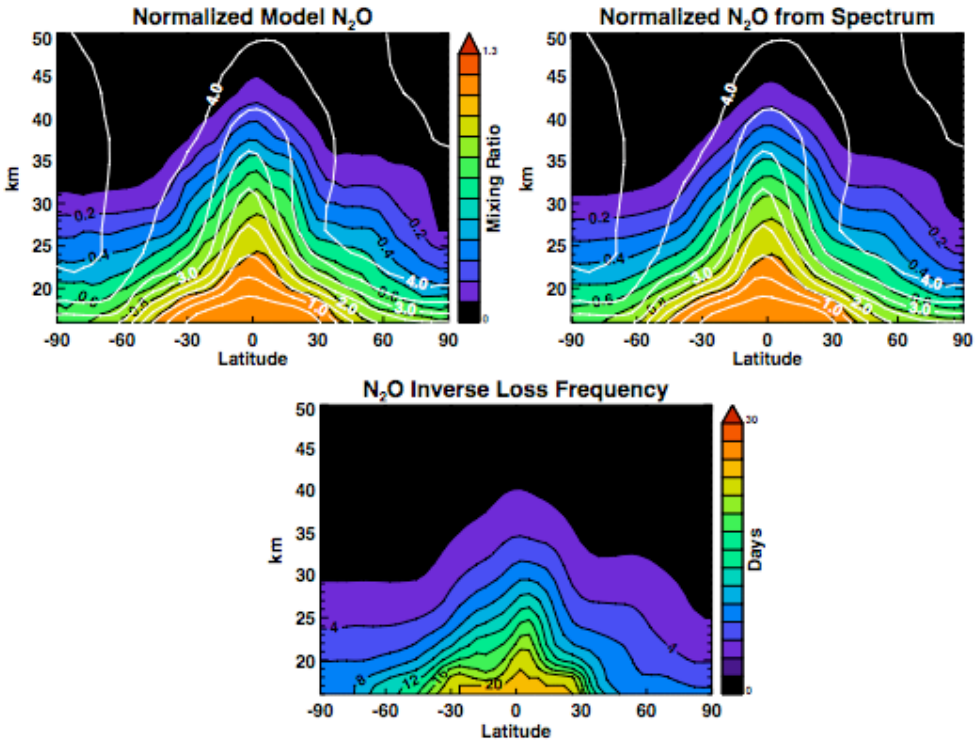

Figure 4b. Same as Fig. 4a but for N_2O.

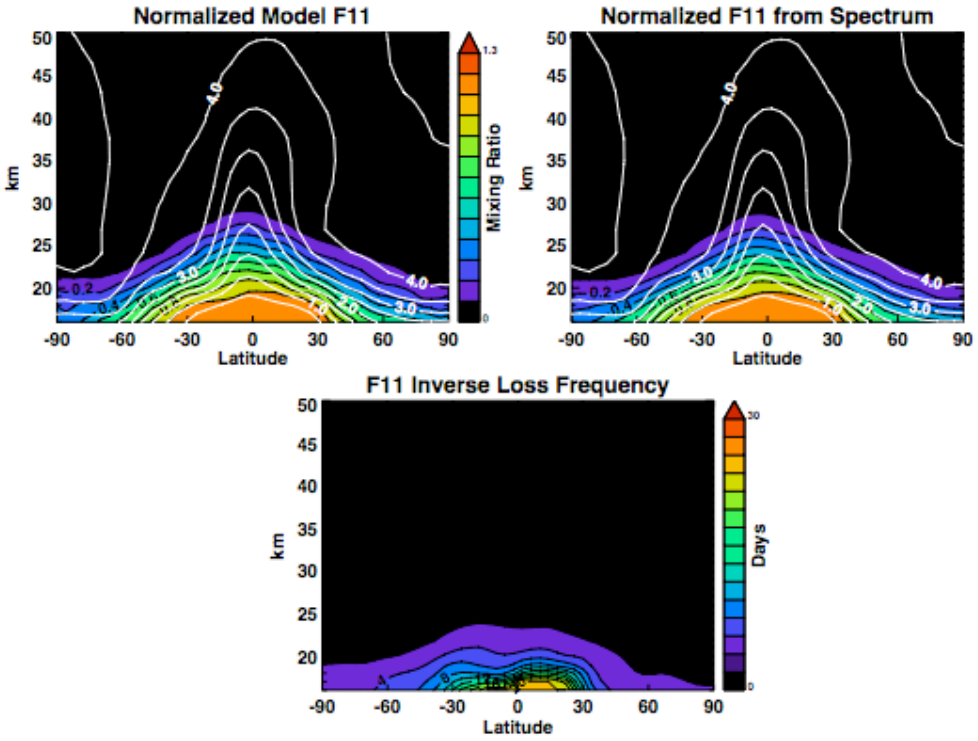

Figure 4c. Same as Fig. 4a but for F11.

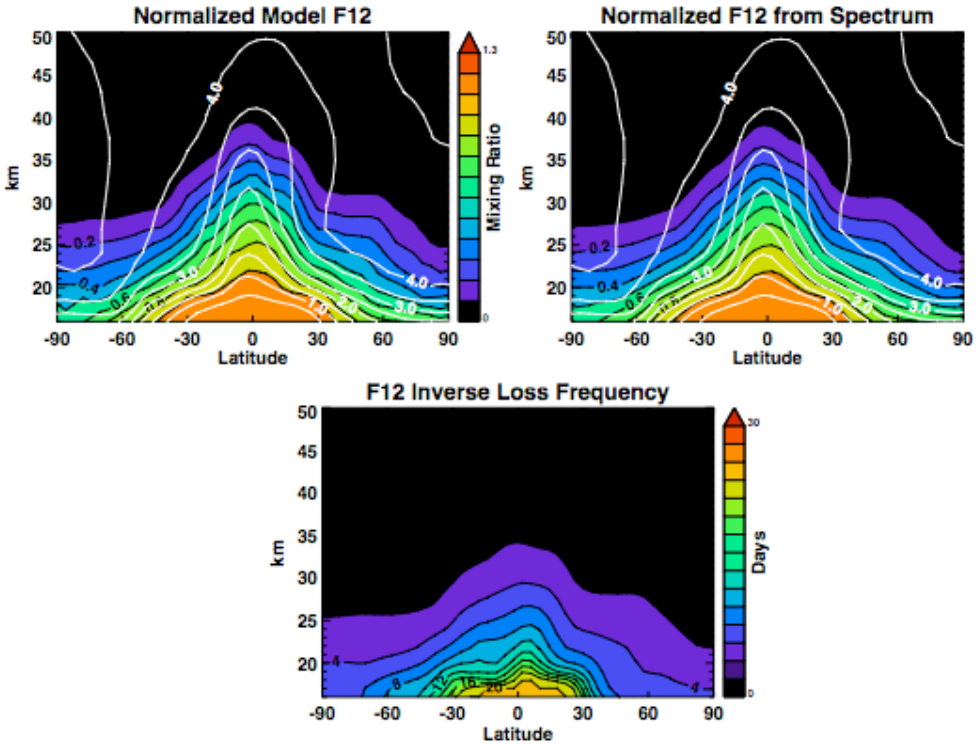

Figure 4d. Same as Fig. 4 but for F12.

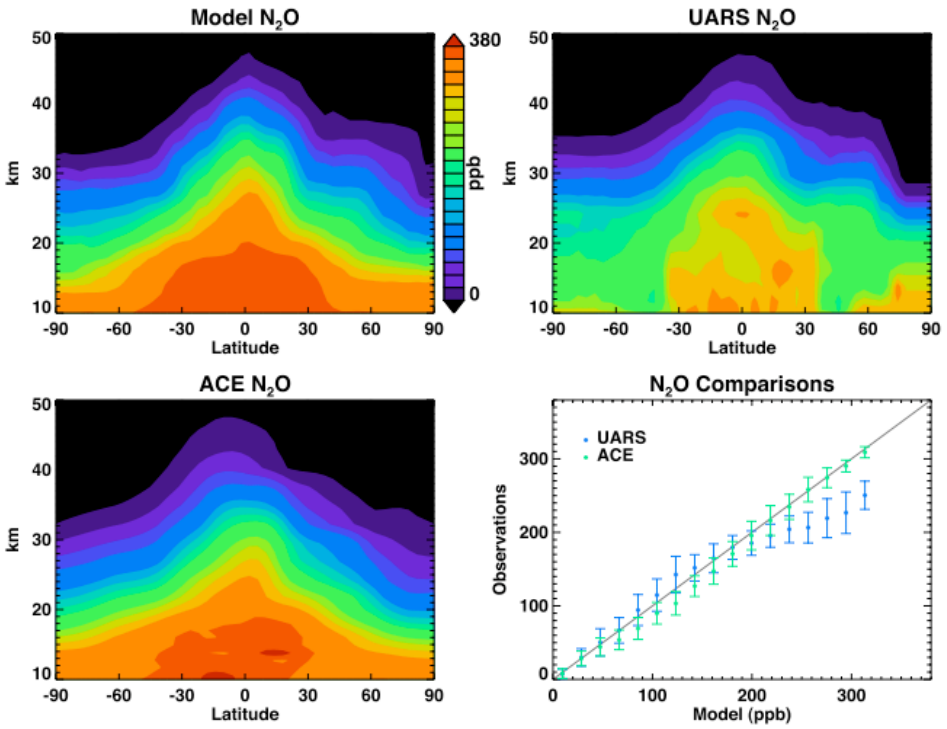

Figure 5a. Upper right, the model zonal mean values of N_2O for January are shown. CLAES observations for January 1993 and ACE observations for Jan 20-Feb. 28, 2005 are also shown. The observations are compared against the model in the lower right hand figure. The error bars indicate one standard deviation.

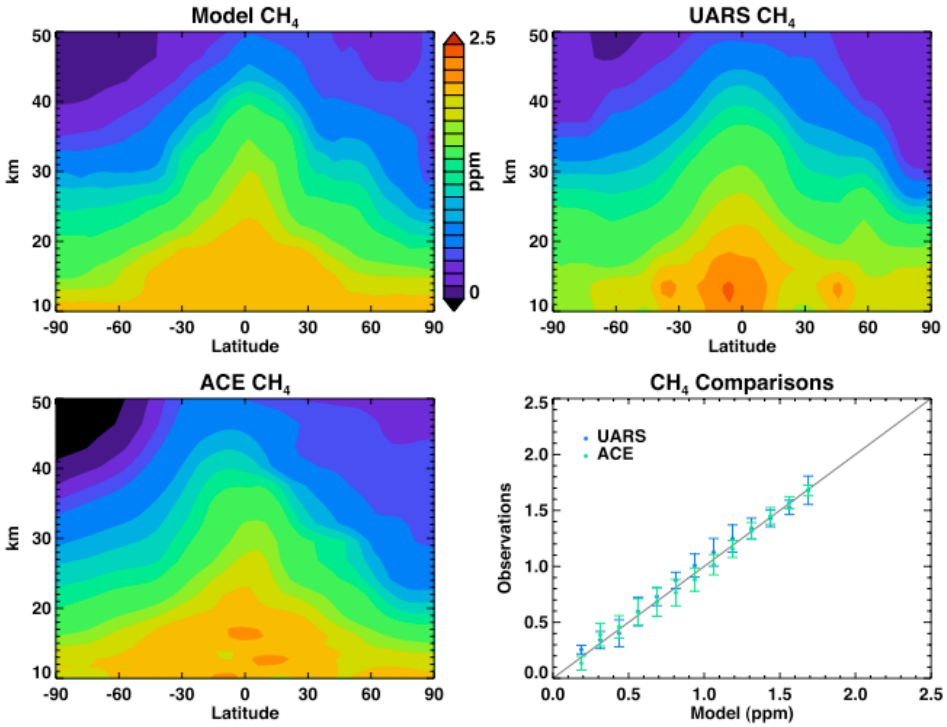

Figure 5b. Same as figure 4a except for methane.

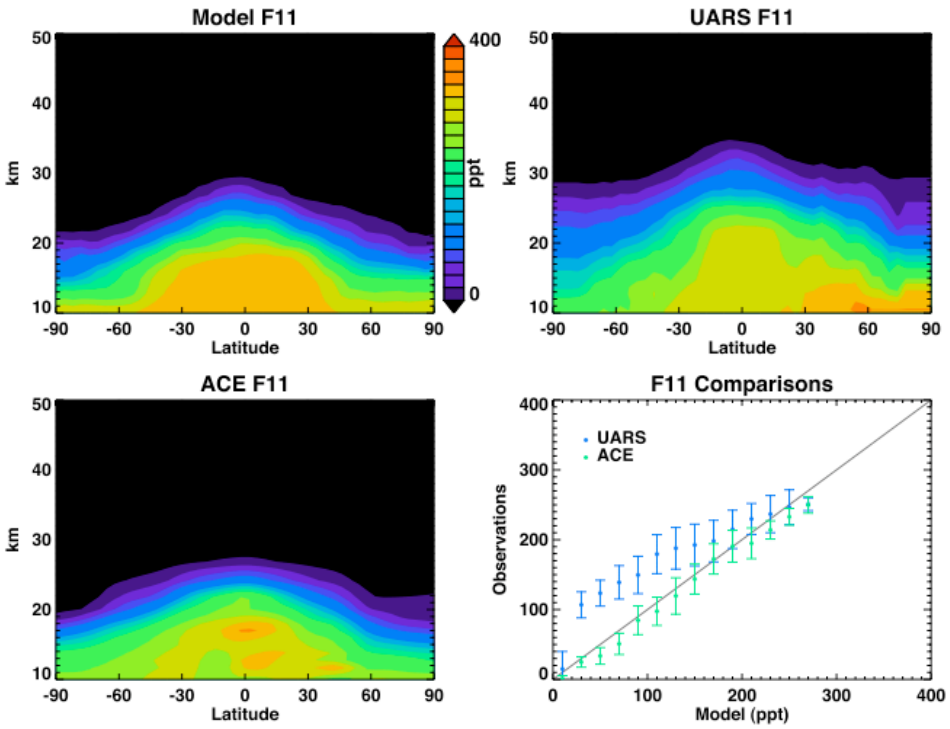

Figure 5c. Same as figure 4a except for F11 (CCl_3F).

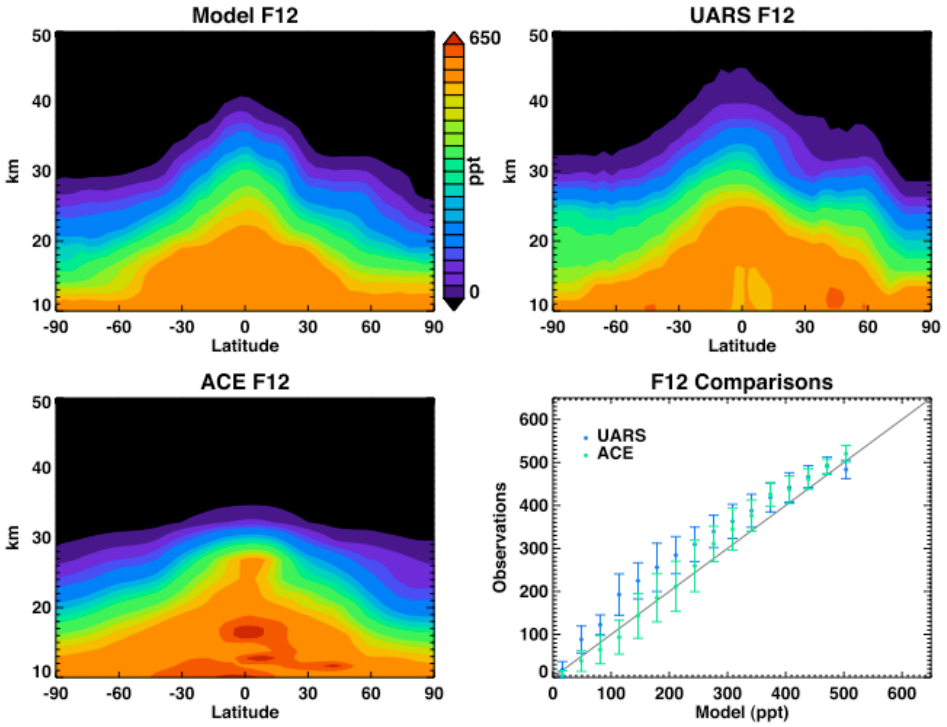

Figure 5d. Same as figure 4a except for F12 (CCl_2F_2).

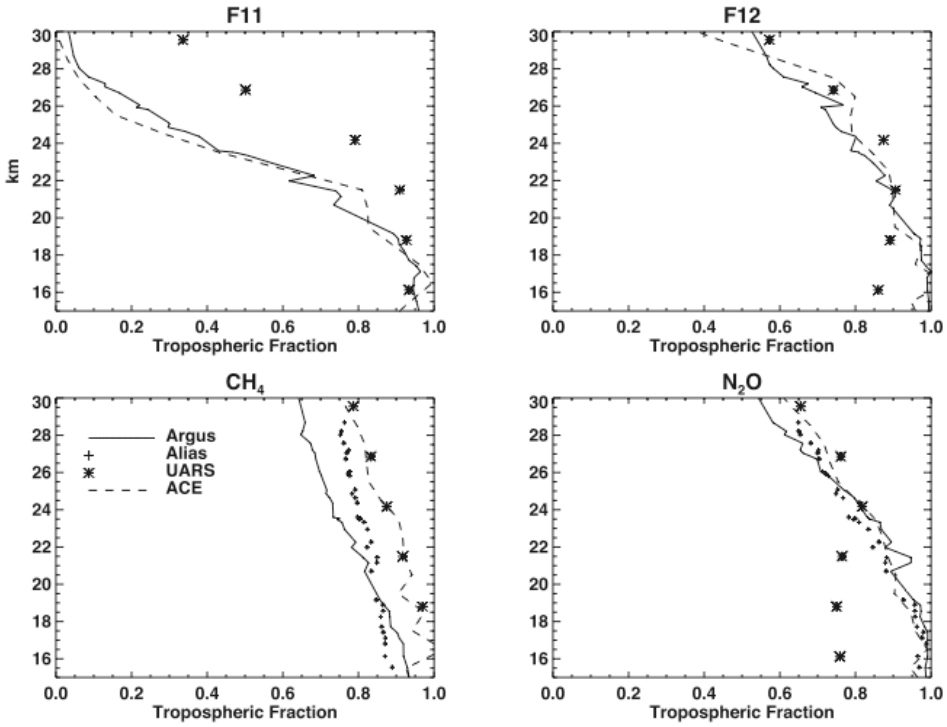

Figure 6a. OMS tropical trace gas profiles as well as ACE and CLAES trace gases normalized to ARGUS tropospheric tracer values.

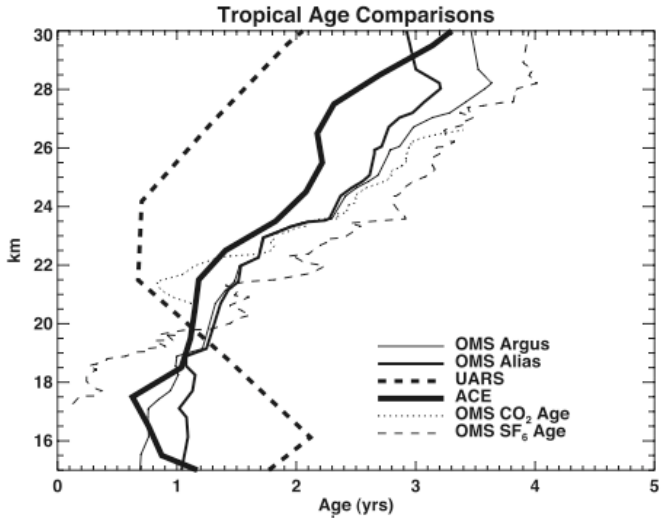

Figure 6b. Ages computed from observations shown in Figure 5a compared with ages from OMS CO_2 and SF_6.

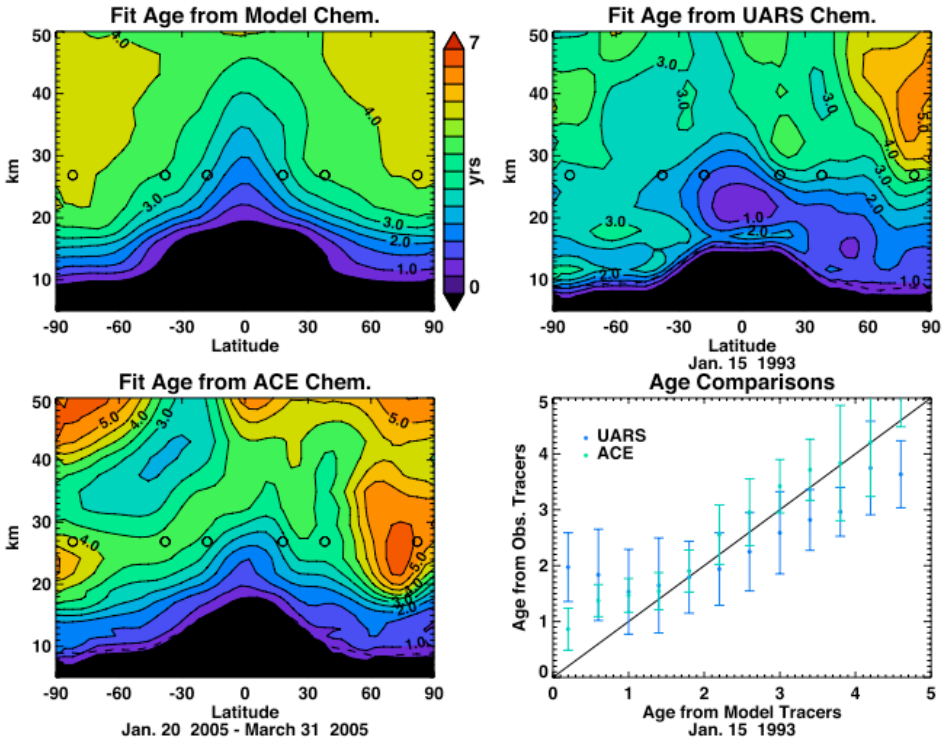

Figure 7. The mean age estimated using the four trace gases in the chemical model (left) and the mean age estimated from the same four tracers using UARS observations (right)

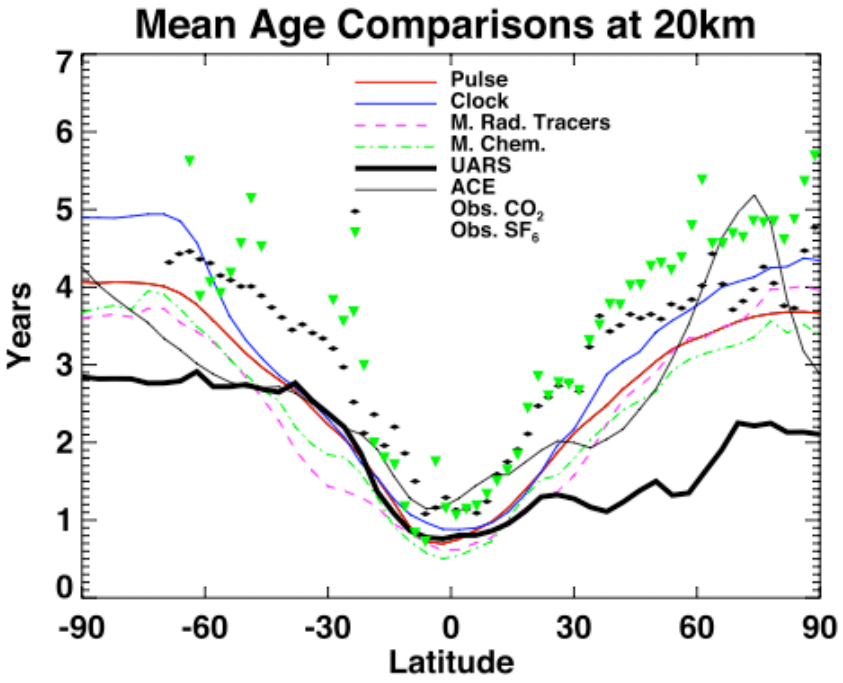

Figure 8. The 20 km mean age computed using the model and observations reported in Waugh and Hall [2002]. Observations are from the clock tracers SF_6 (green) and CO_2 (black) are shown as points. The mean ages are shown as lines for the various experiments, Pulse mean age (red), Clock A tracer (blue), model radioactive tracers (cyan dashed), model chemical tracers (green dashed), UARS CLAES, heavy black, ACE, thin black.

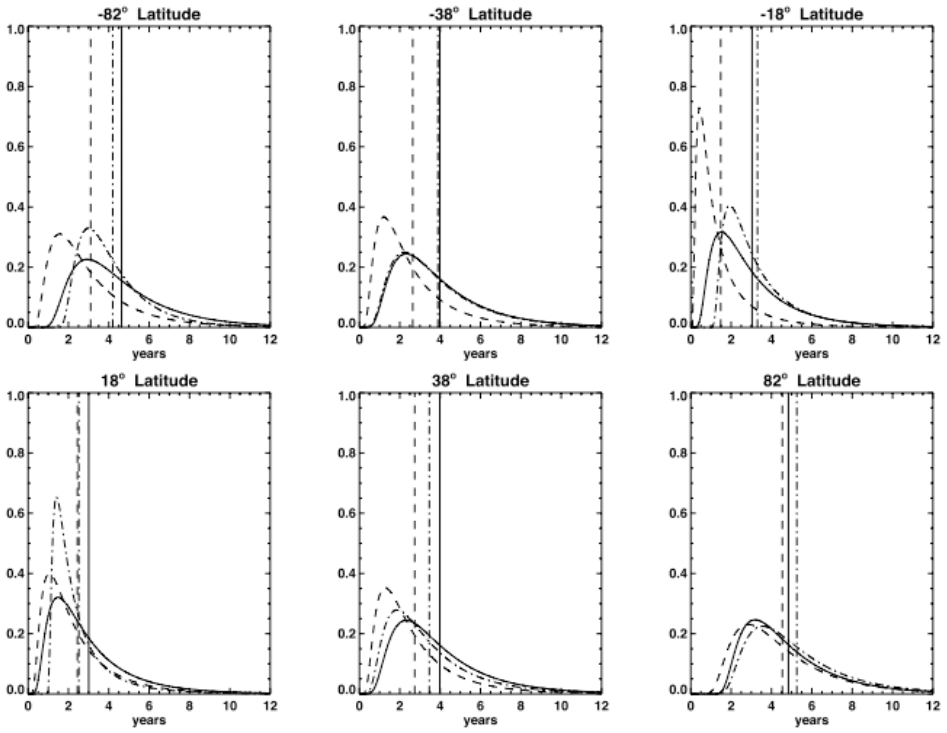

Figure 9. The 30 km age spectrum computed from the model using the four model chemical tracers (solid) and from UARS CLAES data (dashed). The vertical lines show the mean ages. A map of the mean ages is shown in Figure 8.